



Rapid identification and drug susceptibility screening of ESAT-6 secreting *Mycobacteria* by a NanoELIwell assay

Yen H. Nguyen¹, Xin Ma² & Lidong Qin^{1,3}

SUBJECT AREAS:

PATHOGENS

NANOBIOTECHNOLOGY

PATHOLOGY

ENVIRONMENTAL
MICROBIOLOGY

Received
2 May 2012

Accepted
10 August 2012

Published
6 September 2012

Correspondence and requests for materials should be addressed to X.M. (xma@tmhs.org) or L.Q. (lqin@tmhs.org)

¹Department of Nanomedicine, The Methodist Hospital Research Institute, Houston, TX, United States of America, ²Center for Molecular and Translational Human Infectious Diseases Research, The Methodist Hospital Research Institute, Houston, TX, United States of America, ³Department of Cell and Developmental Biology, Weill Medical College of Cornell University, New York, NY, United States of America.

To meet the global needs of tuberculosis (TB) control, a nanoELIwell device was developed as a multifunctional assay for TB diagnosis and drug susceptibility testing. The device integrates on-chip culturing of mycobacteria, immunoassay, and high-resolution fluorescent imaging. *Mycobacterium smegmatis* and *Mycobacterium kansasii* were used as models of *Mycobacterium tuberculosis* to evaluate device integrity by using antigens, Ag85 and ESAT-6, as biomarkers. As a result, the nanoELIwell device detected antigens released from a single bacterium within 24–48-hour culture. Antimycobacterial drug-treated *M. smegmatis* showed significant decreased in Ag85 antigen production when treated with ethambutol and no change in antigen production when treated with rifampin, demonstrating drug susceptibility and resistance, respectively. The nanoELIwell assay also distinguished the ESAT-6-secreting *M. kansasii* from the non-ESAT-6-secreting *M. simiae*. The combination of microwell technology and ELISA assay holds potential to the development of a rapid, sensitive, and specific diagnostics and susceptibility testing of TB.

Tuberculosis (TB), caused by *Mycobacterium tuberculosis* (*M. tuberculosis*), is among the most prevalent and deadliest infectious diseases world-wide, accounting for 9 million new cases and nearly 1.5 million deaths annually¹. Currently, the time-consuming *M. tuberculosis* culture (4–8 weeks) remains the gold standard in the diagnosis of active TB disease as well as the identification of drug-resistance. Smear Acid-Fast Bacilli (AFB) microscopy is the most common, rapid, and inexpensive screening test; however, it has only 53% sensitivity in diagnosis of active TB disease². To date, a rapid and sensitive testing for active TB disease is still highly desirable. Comparative genomic studies have revealed two genes, ESAT-6 (6 kDa early secretory antigenic target gene) and CFP-10 (culture filtrate protein 10 gene) exclusively present in several pathogenic mycobacterial species, including *M. tuberculosis*, and non-tuberculosis species (NTM, *M. kansasii*, *M. szulgai*, *M. marinum*, and *M. riyadhense*)³, and consistently missing from all versions of attenuated vaccine strains (Bacillus Calmette-Guérin, BCG) and most NTM species³. High frequency circulation of CFP-10 and ESAT-6-specific Interferon- γ -secreting CD4 and CD8 T lymphocytes have been detected in patients with active TB disease and latent TB Infection⁴. Based on these findings, two ESAT-6/CFP-10-based immunodiagnostic kits, T-SPOT®. TB and QuantiFERON® TB, have been commercialized to detect *M. tuberculosis* infection. Both of these host-immunity-based tests, however, have failed in distinguishing between active TB disease and remote latent TB infection (LTBI) due to the immunologic response from long-lived human memory T cells⁵. The molecular basis of drug resistance in *M. tuberculosis* has been studied extensively, with the primary gene mutations associated with TB resistance to the five first-line drugs and the four second-line drugs already identified⁶. The convergence of global data on TB infections has shown, however, that these known gene mutations cannot explain all of the drug resistant phenotypes, indicating more drug-resistant gene mutations remain as yet undiscovered. Time-consuming culture-based testing remains the standard for *M. tuberculosis* drug resistance identification.

Microwell technology^{7–10} has been designed to better confine cells into nanoliter volumes for single cell analyses, including cytokine sensing^{11,12}, measurements of antigen production rates^{13,14}, multiple-antibody



characterization¹⁵, and general single-cell trapping^{16,17}, culture^{18,19}, and content^{20–22}. The enzyme-linked immunosorbent assay (ELISA) and microwell technologies have been combined to analyze the cytokine panels of immune cell response^{10,14,16,23}. The major advantage of these combined technologies is to significantly increase the sensitivity and shorten the analytical time by confining the cytokines released from cultured cells within a nanoliter chamber for ELISA assay. In this study, we design a mycobacteria antigens-based nanoELIwell device for rapid mycobacterial identification and drug resistance screening. Our data has shown that this device can successfully culture mycobacteria in a nanoliter chamber and analyze the antigen secretion within 48 hours, which provides an ideal platform for further development of rapid diagnosis of active TB disease.

Results

NanoELIwell design. In order to effectively isolate and confine mycobacteria, the nanoELIwells were designed to have either a $50 \times 50 \mu\text{m}$ (154,100 ELIwells/slide, ~ 0.025 nanoliter per well) or $100 \times 100 \mu\text{m}$ (34,825 ELIwells/slide, ~ 0.1 nanoliter per well) dimensions, an area small enough to contain sufficient media for the culturing of one to a few bacteria per nanoELIwell (Figure 1). The device was fabricated using standard photolithography techniques²⁴ that employs elastomeric poly(dimethylsiloxane) (PDMS) as the cast on silicon SPR mold, giving rise to a depth of approximately $10 \mu\text{m}$ that is enough to contain a single layer of bacteria. The length and width of the nanoELIwells can be sized accordingly to the

experiment. As many as 30 small pieces of PDMS nanoELIwells, each under different conditions, can be mounted onto a single standard microscope glass slide for high throughput analyses. The glass slides are coated with epoxides and then functionalized with the desired antibodies 12 hours prior to bacterial culture. The mycobacteria were separated from the liquid culture media through multiple centrifugation/washing steps with fresh Middlebrook 7H9 Broth media prior to installation onto the nanoELIwell. This step was critical for the removal of any existing antigens from the media, resulting in a clear black background in the fluorescent assays. A $10 \mu\text{L}$ of Middlebrook 7H9 Broth media containing mycobacteria was added onto nanoELIwells, that were either pretreated with a fibronectin soak or a three minute oxygen plasma cleaning session. This step generated a hydrophilic surface for a better media installation into the nanoELIwells. Afterwards, an antibody-coated glass slide was mounted onto the nanoELIwells (Figure 1), then sandwiched by two acrylic plates with 4 screws (Figure 1A). The whole device was placed inside a biosafety container and cultured for 24–48 hours at 37°C . At the end of the bacteria culture, the sandwich was dismantled by carefully separating the nanoELIwells from the glass slide. The bacteria-containing nanoELIwells were then vacuum dried for scanning electron microscope (SEM) imaging, while the glass slides were assayed for fluorescence imaging. Herein, SEM imaging is to confirm bacterial presence, which will not be needed for future clinical applications. The experimental details are described in the Methods Section.

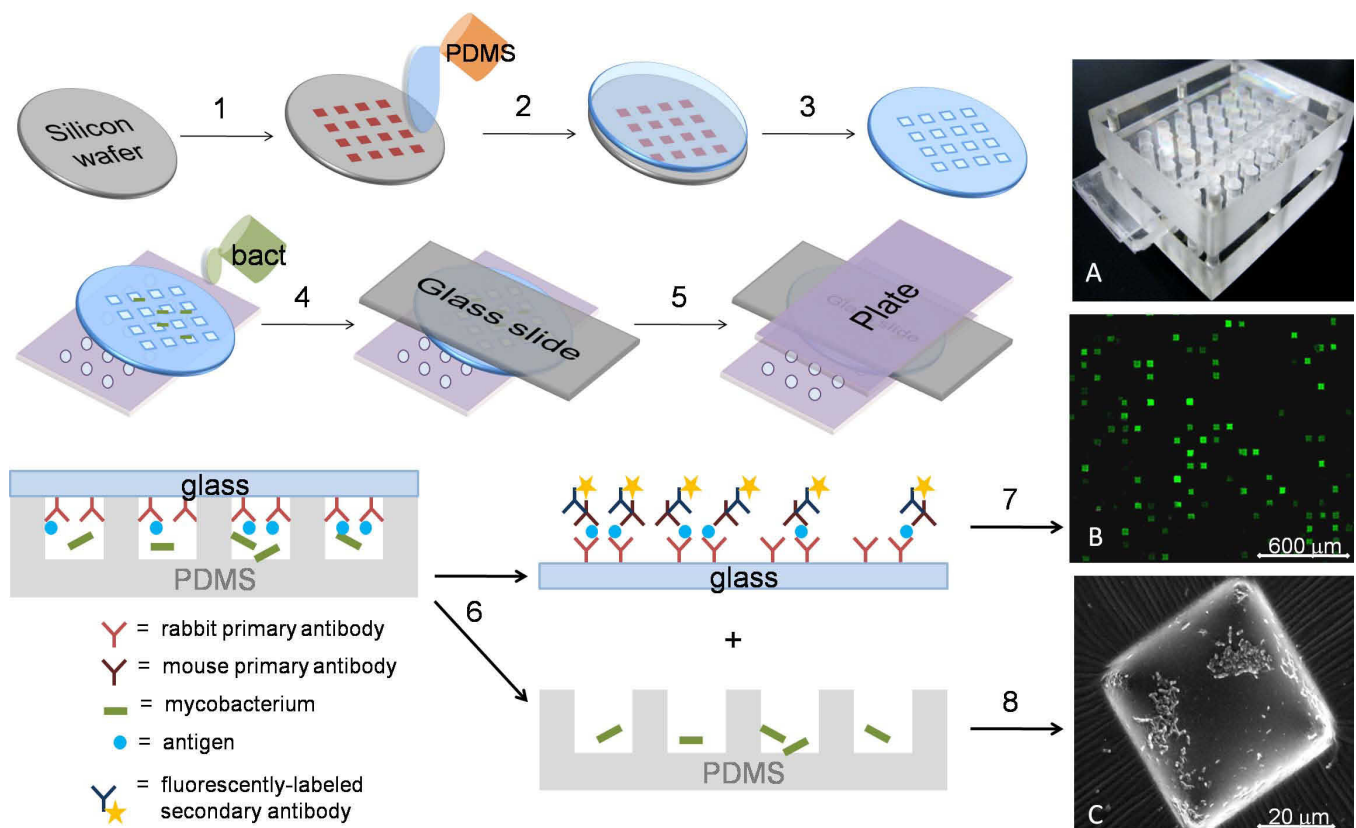


Figure 1 | Design scheme. (1) The nanoELIwell master was fabricated using silicon wafers and standard rapid prototyping techniques. (2) PDMS soft photolithography was employed to generate the elastomeric nanoELIwells for bacterial cultures. (3) The PDMS was then peeled off from the master and sized if needed before each experiment. The nanoELIwells were then placed on top of an acrylic plate with holes, which allow for the delivery of oxygen/ CO_2 during culture. (4) Bacteria were deposited onto oxygen plasma-treated or fibronectin-soaked nanoELIwells and covered by the antibody-coated glass slide. (5) The device was then held together with a second acrylic plate (without holes) and cultured for 24–48 hours at 37°C (as shown in Figure A) before being dismantled for analysis. (6) The glass slide was carefully removed without disturbing the bacteria in the nanoELIwells. (7) The ELISA assay was conducted with a fluorescently-labeled secondary antibody and imaged using a microarray scanner (Figure B). (8) The nanoELIwells PDMS stamp were completely dried under a vacuum, coated with a thin layer of gold, and imaged using SEM techniques (Figure C).



Evaluation of NanoELIwell device with *M. smegmatis* and antigen Ag85. To evaluate the function of the nanoELIwell in detection of mycobacteria biomarkers, *M. smegmatis*, a non-pathogenic laboratory model for *M. tuberculosis*, and its secreted antigen Ag85 was first used in this study^{25,26}. The culturing procedure and the device preparation are described in the Methods Section. The Ag85 antibody-coated glass slide was fluorescently imaged (Figure 2A and B) while the PDMS layer was characterized by using SEM techniques (Figure 2C). As shown in the fluorescent data (Figure 2A and B), each nanoELIwell has varying fluorescence signal intensities, indicating different bacterial loads and/or varying Ag85 antigen secretion rates in different nanoELIwells. The fluorescence intensities in nanoELIwells were correlated with the bacterial loads, which was evidenced by aligning the fluorescent images with the bacteria SEM images of each nanoELIwell (Figure 2C). To better understand the correlation between the bacterial load and the fluorescence signal density/intensity in the nanoELIwell, *M. smegmatis* culture specimens were diluted with a gradient of 1x (1.4×10^5 bacilli), 5x (2.8×10^4 bacilli), and 10x (1.4×10^4 bacilli) and were cultured in the nanoELIwells with Ag85 antibody-functionalized glass slide for 24 hours. As expected, the fluorescence intensities/densities on the glass slides were highly correlated with the bacterial loads in the nanoELIwells. Importantly, when a single bacterium was cultured and found in a single nanoELIwell by SEM (Figure 3C), its fluorescence signal was still detectable (Figure 3F), which clearly indicates the detection limit down to a single mycobacterium. A single-cell detection limit was further investigated against AFB microscopy (Figure 4). SEM images of a diluted sample of bacterial culture (200 bacilli over a 3×3 mm scanned area) were collected (Figure 4A and B) and correlated with its fluorescence assay (Figure 4C) directly indicating single-cell analysis capabilities. This result was compared directly to AFB microscopy against both Morse fluorescence stain (Figure 4D) and Ziehl-Neelsen stain (Figure 4E) techniques, however, samples had to be concentrated by 100x in order for signal to be visible using the standard microscopy protocols. There is little to no signal present for the sample (Figure 4D, large oval) compared to the positive control (Figure 4D, lower left circle) using the Morse fluorescent stain; this method was concluded not to be the appropriate method for bacterial detection at this low of a concentration for *M. smegmatis* detection. The same sample concentration was used in Figure 4E using the Ziehl-Neelsen stain, a method previously shown to be an appropriate method for staining *M. smegmatis*^{27,28}. A few bacilli were indeed visible under the 40x microscopic lens; however the blue color is not as easily detectable compared to our nanoELIwell results. To demonstrate the nanoELIwell sensitivity against AFB standard protocols, the same sample was diluted by 100x (down to approximately 200 bacilli

over the scanned area) and cultured using our nanoELIwell technology, fluorescently assayed, and imaged (Figure 4F). As indicated, fluorescent signal was still present even at 100x dilution, therefore demonstrating approximately 100 fold increase in sensitivity to standard AFB microscopy. Furthermore, the bacteria are confined and localized within a 50x50 micron well using our nanoELIwell device, resulting in a clear signal readout. Though at a low bacterial concentration, the fluorescent signal is still visible for easy readout. Single-cell bacterial confinement allows for increase sensitivity in nanoELIwell assays.

Drug susceptibility and resistance testing by the nanoELIwell device. To evaluate the capability of the nanoELIwell device in the detection of mycobacterial drug susceptibility, *M. smegmatis* was pre-incubated for 1 hour in liquid media containing ethambutol (EMB, 8 $\mu\text{g}/\text{mL}$)^{29,30}, then placed into nanoELIwells with the Ag85 antibody-coated glass slides. EMB-untreated *M. smegmatis* was mounted onto the same antibody-coated glass slide as the EMB-treated sample. After 24-hour culture, the untreated *M. smegmatis* showed substantial Ag85 antigen secretion with intensive fluorescence signals as expected (Figure 5A), while the EMB-treated *M. smegmatis* presented significantly weaker fluorescent signals (Figure 5B), indicating much lower production of the Ag85 antigens compared with the untreated bacteria. Ethambutol is a bacteriostasis drug that inhibits bacterial growth^{31,32}. This becomes evident by the decrease in Ag85 production, as seen by a lower fluorescent signal in Figure 5B than Figure 5A. Drug resistance was then explored using rifampin (RIF, 1 $\mu\text{g}/\text{mL}$)^{33,34} following the same protocol as stated above, however a significantly more diluted sample was used for single cell analysis. The concentration of 1 $\mu\text{g}/\text{mL}$ was chosen for the experiment because the MIC of RIF has been previously reported to be 4 $\mu\text{g}/\text{mL}$ ³⁵. A concentration above the MIC will result in a susceptible response from *M. smegmatis*. The RIF-untreated sample (Figure 5C) showed the same signal profile as the RIF-treated sample (Figure 5D), evidenced by the same fluorescent intensity/density; thus, indicating that *M. smegmatis* has a resistant response to RIF treatment at that concentration. This data clearly justified the applicable potential of the nanoELIwell device for rapid identification and screening for antimycobacteria drug resistance and susceptibility properties.

NanoELIwell assay for ESAT-6 secreting mycobacteria. The ESAT-6 antigen is secreted by several pathogenic mycobacterial species, including *M. tuberculosis* and *M. kansasii*. In this study, *M. kansasii* was utilized as a laboratory model of ESAT-6 secreting mycobacteria, while *M. simiae* (a non-ESAT-6 secreting species) was used as a control^{3,36}. Both *M. kansasii* and *M. simiae* are slow-growing non-tuberculosis mycobacteria (NTM). The *M. kansasii*

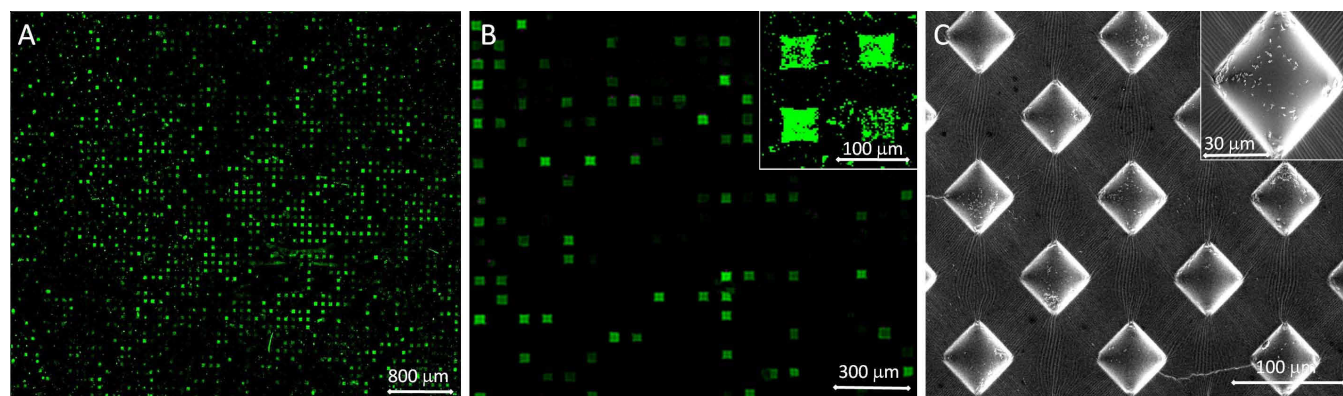


Figure 2 | *M. smegmatis* analysis. (A and B) Fluorescent images of Ag85 antigen detected from a 24-hour nanoELIwell culture of *M. smegmatis* and (C) SEM images of nanoELIwells containing *M. smegmatis*. There were approximately 28,000 bacterial cells over the scanned area (5x5 mm). (Insets are zoomed-in images).

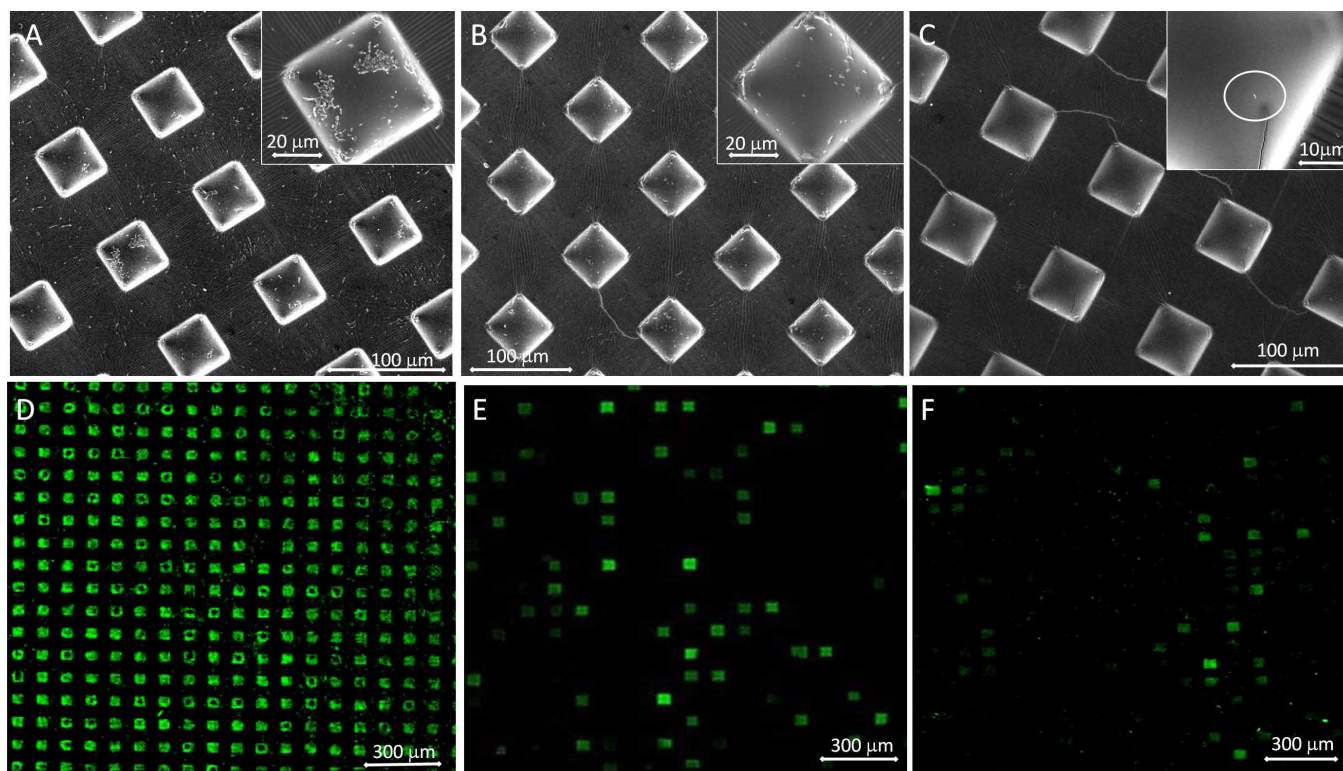


Figure 3 | Sensitivity assays of nanoELIwell culture of *M. smegmatis*. (A–C) SEM images of *M. smegmatis* on nanoELIwells in 3 dilution gradients; A/D: 1x (1.4×10^5), B/E: 5x (2.8×10^4), C/F: 10x (1.4×10^4) over a 5x5 mm scanned area. The insets show zoomed-in images of the individual nanoELIwells (50x50 μm), which demonstrate the amount of bacteria for each culture. (D–F) Scanning fluorescence data of the respective nanoELIwell showed above, visually demonstrating the correlation between the fluorescent signal density/intensity and bacterial loads in each nanoELIwell.

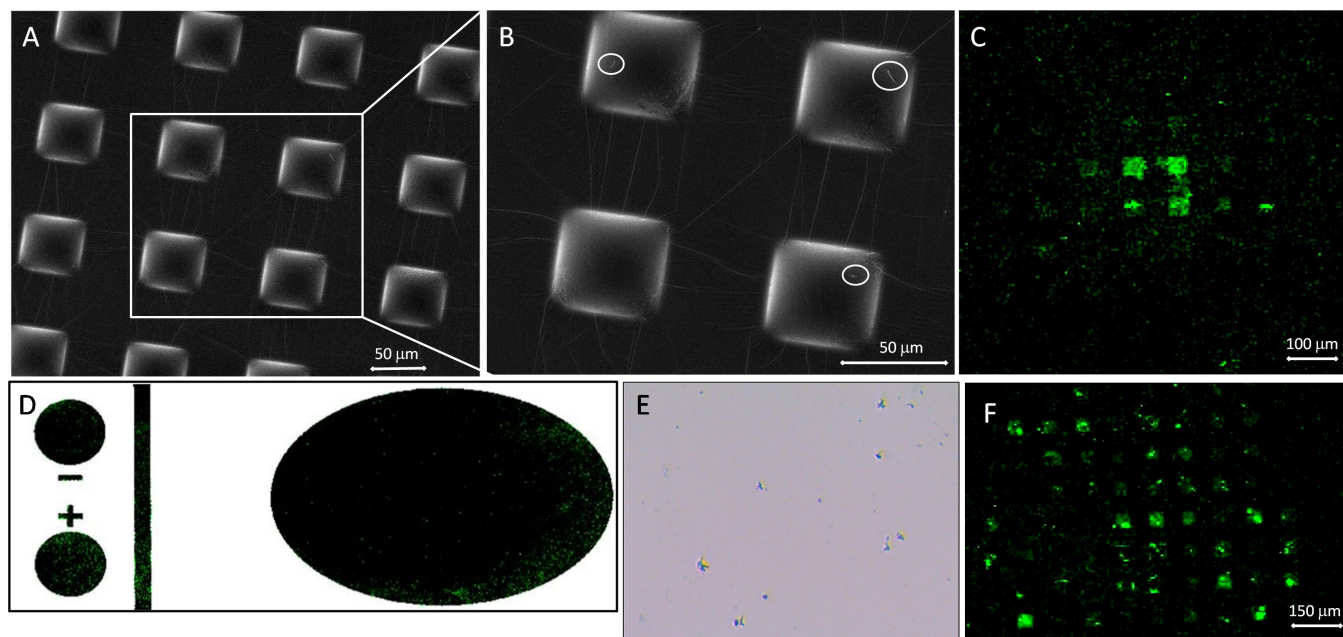


Figure 4 | Detection limit of nanoELIwell technology down to single-cell level. (A) SEM image of *M. smegmatis* at a low concentration, 200 bacilli over a 3x3mm scanned area of nanoELIwells. (B) A zoomed-in SEM image highlighting the single bacterium in each nanoELIwell. (C) Scanning fluorescence data of nanoELIwell of samples from (A)/(B), visually demonstrating the correlation between the fluorescent signal density/intensity and bacterial loads in each nanoELIwell. (D) AFB fluorescence smear (Morse stain) demonstrating poor signal quality even for the positive control in the lower left of the slide. Samples of *M. smegmatis* in the larger oval are undetectable at this concentration using this method. (E) AFB smear microscopy (Ziehl-Neelsen stain) at 40x magnification. (F) Scanning fluorescence data of a sample that is 100x more diluted than samples in D and E, demonstrating that the nanoELIwell technology has a detection limit that is at least 100-fold more sensitive than AFB microscopy, which calculated to be roughly 200 bacterial cells per sample load.

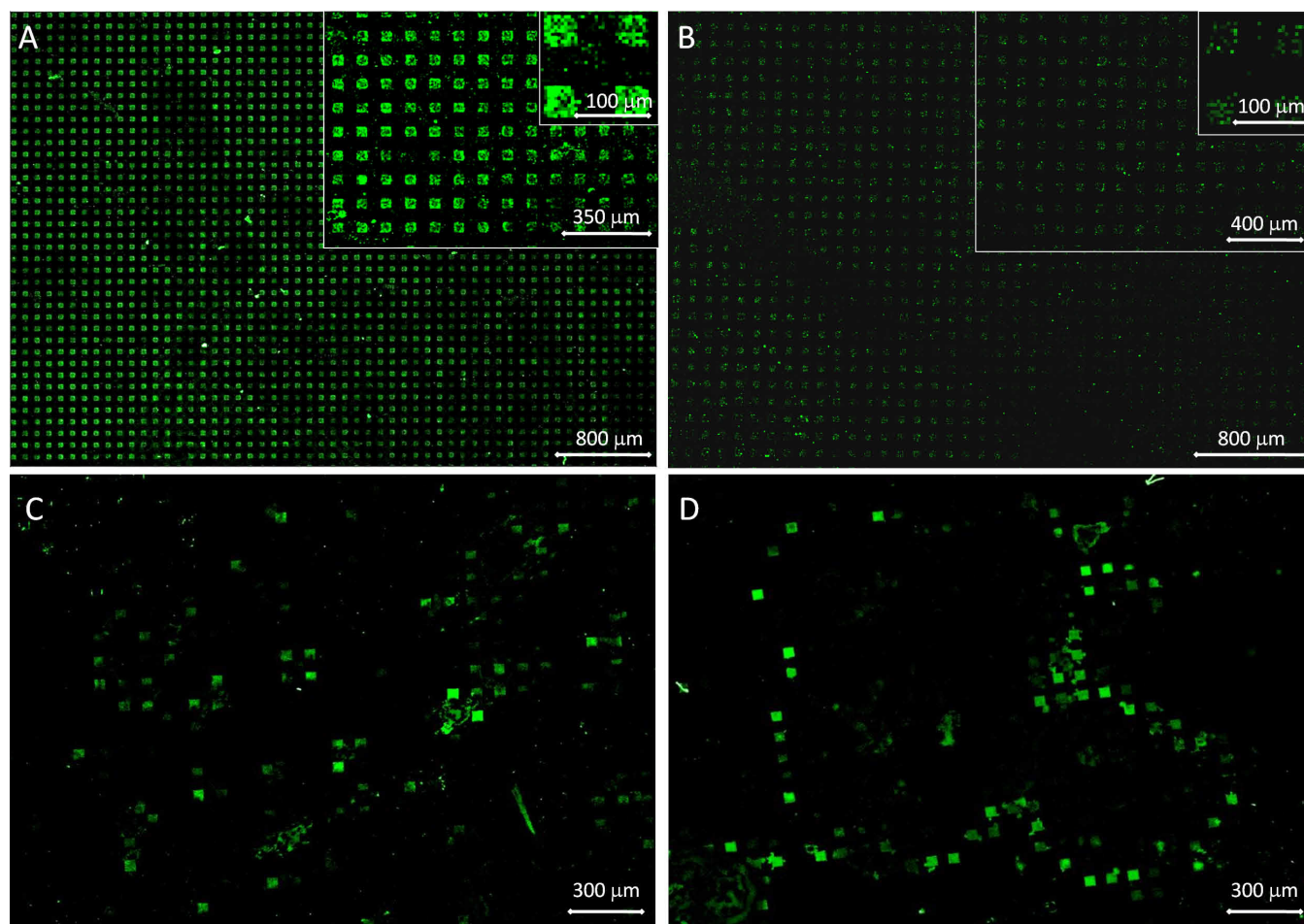


Figure 5 | Drug susceptibility and resistance assays. Fluorescence data of (A) EMB-untreated and (B) EMB-treated (8 $\mu\text{g/mL}$) *M. smegmatis* cultured in ELIwells for 24 hours. The insets are zoomed-in images. Each ELIwells are $50 \times 50 \mu\text{m}$. The lack of detectable fluorescence in (B) indicates no release or little release of antigens due to bacterial stasis. Fluorescence data of (C) RIF-untreated and (D) RIF-treated (1 $\mu\text{g/mL}$) *M. smegmatis* cultured in ELIwells for 24 hours. Each ELIwells are $50 \times 50 \mu\text{m}$. The lack of detectable difference in fluorescence intensity between (C) and (D) indicates bacterial resistance to rifampin treatment.

and *M. simiae* were cultured in two separate nanoELIwell devices with ESAT-6 antibody-functionalized glass slides for 48 hours. The fluorescence data revealed the secretion of ESAT-6 antigen from *M. kansasii* with intensive signals (Figure 6A), while no ESAT-6 antigens were detected from *M. simiae* (Figure 6E). The SEM images for *M. kansasii* (Figure 6 B–D) and *M. simiae* (Figure 6 F–H) showed the bacterial presence in both nanoELIwells. This data clearly indicates that the ESAT-6-based nanoELIwell device is able to identify ESAT-6 secreting mycobacteria within a short culture time, which holds a great potential to develop a rapid screen test for active TB disease with a higher sensitivity and specificity compared with the traditional AFB smear microscopic test.

Discussions

TB, especially drug resistant TB disease, remains on the top of public health concerns globally. Rapid identification and drug susceptibility testing of TB disease is one of the priorities among global TB control efforts. Our study aims to meet these needs by utilizing latest microwells and immunoassay technologies. Results from this study has shown that the nanoELIwell device, designed by combining microwells and ELISA technologies, successfully integrates four advantages together, including rapid culturing of slow-growing mycobacteria, a high specificity with antigen-based immunoassay, a high sensitivity (single mycobacterium detection) with high-resolution fluorescence scanning of up to 154,100 ELIwells per slide,

and a rapid screening of drug resistance/susceptible of mycobacteria. These advantages hold a great potential towards the development of a high throughput/automatic identification assay of active TB disease and anti-TB-drug resistance/susceptibility.

A limitation of this ESAT-6-based nanoELIwell is that several pathogenic mycobacteria species secrete ESAT-6 antigen, which may lower the specificity for TB diagnosis. *M. kansasii*, the most common ESAT-6-releasing NTM can cause a chronic pulmonary infection that resembles pulmonary tuberculosis. *M. kansasii* infection is the second-most-common nontuberculous opportunistic mycobacterial infection associated with AIDS, surpassed only by *M. avium* complex (MAC) infection^{37,38}. Additional methods, e.g. 16S rRNA gene sequence analysis will be needed for species identification of pathogenic mycobacteria in the immunocompromised patients. However, in countries with high TB prevalence, like China, the *M. kansasii* accounts for approximate 0.12% of pulmonary TB suspects without HIV/AIDS³⁹. Therefore, the ESAT-6-based nanoELIwell assay still has a relatively higher specificity compared with the conventional TB diagnostic assays. Further clinical evaluation of the nanoELIwell device with *M. tuberculosis* will be able to confirm its capability and lead to applications in diagnostic practice.

Methods

Materials. SuperEpoxy2, Protein Printing Buffer, Washing Buffer, Rinsing Buffer, Reaction Buffer, BlockIT, and the Microarray High-Speed Centrifuge used for microarray analysis were purchased from ArrayIt (Sunnyvale, CA, USA). The

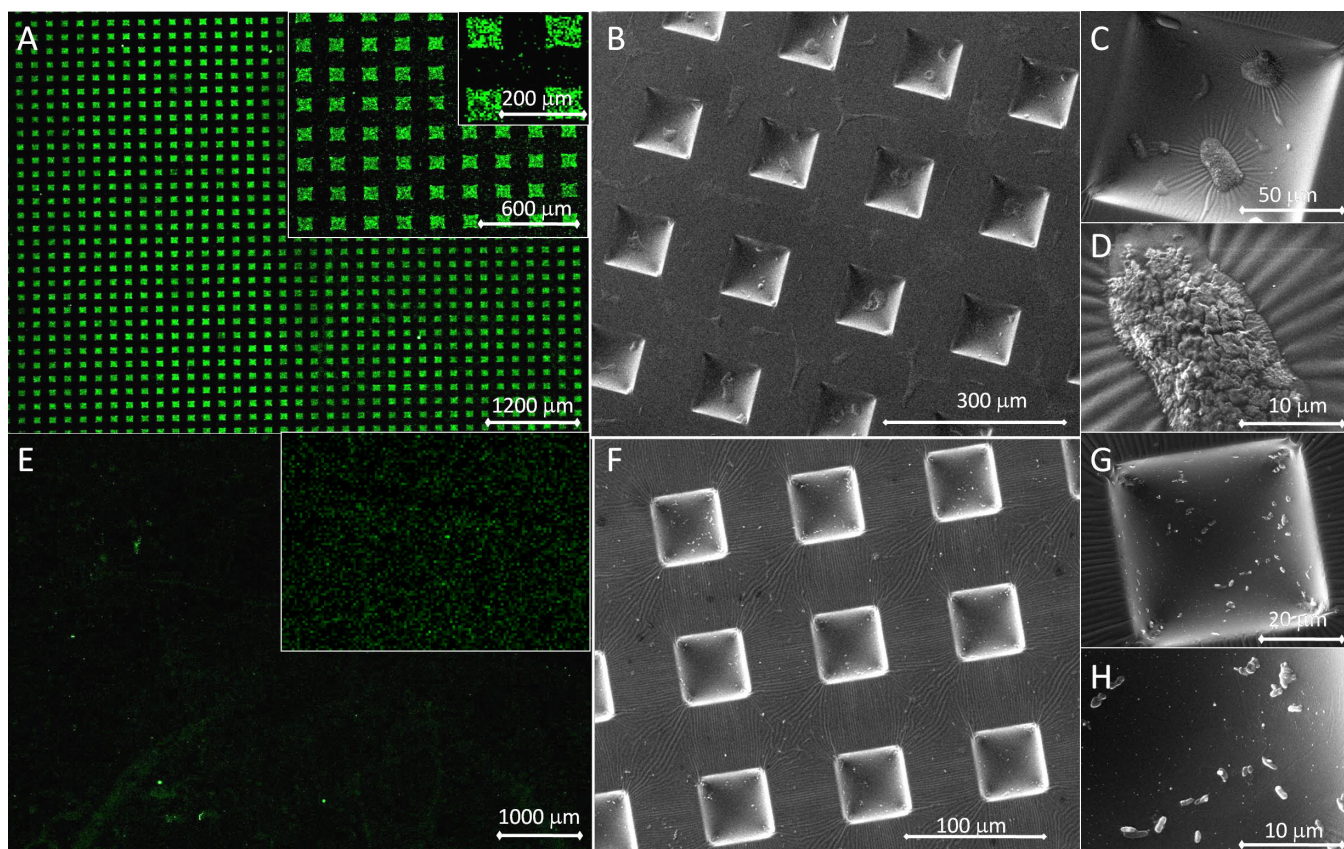


Figure 6 | NanoELIwell distinguishing assay for ESAT-6 secreting Mycobacteria. EAST-6 secreting *M. kansasii* presented intensive signals on NanoELIwells coated with ESAT-6 antibody (A), but no signal from non-ESAT-6 secreting *M. simiae* (E) from a 48 hour nanoELIwell culture, insets are zoomed-in images. The inset in (E) displays 5 μm resolution pixels of the microarray scanner limit, indicating only background noise and no detectable signal. SEM images (B–D) of nanoELIwells contained *M. kansasii* in 100x100 μm ELIwells and SEM images (F–H) contains *M. simiae* in 50x50 μm ELIwells.

hybridization chambers used for antibody loading were purchased from Corning Incorporated (Lowell, MA, USA). Megaposit SPR 220-7 positive photoresist and Microposit MF-CD-26 Developer were obtained from Rohm and Haas Electronic Materials (Midland, MI, USA). RTV 615 poly(dimethylsiloxane) (PDMS) were purchased from Momentive (Columbus, OH, USA). All antibodies (ESAT-6, AG85, and Mouse IgG-Cy3) were purchased from Abcam (Cambridge, MA, USA). High resolution photomasks were designed using AUTOCAD by Autodesk (San Rafael, CA, USA) and were printed onto high-resolution chrome transparencies by Photo-science Incorporated (Torrance, CA, USA). Trimethylchlorosilane (TMCS), hexamethyldisilazane (HMDS), and AFB control and test slides were purchased from Fischer Scientific (Pittsburg, PA, USA). Lowenstein-Jensen agar slants, Middlebrook 7H9 Broth media, Ziehl-Neelsen stain kit, and Morse stain kit, ethambutol, and rifampin were purchased from BD Biosciences (Sparks, MD, USA). *M. smegmatis* was purchased from ATCC (Manassas, VA, USA). *M. kansasii* and *simiae* were from Molecular TB Laboratory, Department of Pathology and Genomic Medicine, The Methodist Hospital Research Institute (Houston, TX).

Device fabrication. The 38,525 (100 μm x 100 μm) and 154,100 (50 μm x 50 μm) nanoELIwell arrays were generated by using AutoCAD (AutoDesk), and printed onto mask transparencies. Based on the standard rapid prototyping techniques⁴⁰, The masters were fabricated by using hexamethyldisilazane-treated silicon wafers that was spin coated (1500 rpm, 40 s) with Megaposit SPR 220-7 positive photoresistant materials, up to a 10- μm thickness. The silicon wafers were soft baked and irradiated with UV light rendering the exposed photoresistant materials soluble in Microposit MF-CD-26 Developer. After washing and drying, the silicon masters were treated with an anti-adhesive agent, trimethylchlorosilane (TMCS), via vapor reaction for one hour. NanoELIwells were prepared from RTV 615 poly(dimethylsiloxane) (PDMS) using soft photolithography techniques²⁴. The base and curing agents were mixed (10:1) by weight, degassed in a vacuum chamber, and cured (80 $^{\circ}\text{C}$ for 1 hour). The nanoELIwell arrays were cut and removed from the masters directly before experimentations.

Functionalization of capture antibody on glass surface. The SuperEpoxy 2 epoxide-coated glass slides were incubated with 100 μL of 2 $\mu\text{g}/\mu\text{L}$ antibodies suspended in Protein Printing Buffer via a hybridization chamber at 4 $^{\circ}\text{C}$ overnight. The following day, the functionalized slides were washed with Washing Buffer and Rinsing Buffer

before incubating in 10 mL Blocking Buffer at room temperature for 4 hours. After blocking, the slides were washed again and rinsed before bacterial loading and culturing.

Bacterial loading and culturing. The nanoELIwells were either oxygen plasma treated or fibronectin soaked directly before bacterial loading. Depending on the experiment, the PDMS can be guillotined down to the desired size for high-throughput assays in as many as 1 to 30 different conditions all on a single functionalized glass slide.

In a typical on-chip test, a 10 μL -culture sample of mycobacterium was collected and centrifuged. The bacteria were washed 3 times with fresh Middlebrook 7H9 Broth media to remove the existing antigens. Afterwards, 3–10 μL of bacterial re-suspensions were dropped directly into the center of the pretreated nanoELIwells and allowed the bacteria to settle into the wells for 3 minutes, before the functionalized glass slides were then placed on top of the nanoELIwells. The nanoELIwells and glass slides were sandwiched between two acrylic plates and held by 4 screws. The sandwiched devices were placed into humidified culture plate and cultured in an incubator at 37 $^{\circ}\text{C}$ (5% CO_2) for 24–48 hours.

Fluorescence analysis. Each sandwiched devices were carefully dismantled by lifting the glass slides off of the nanoELIwells without disturbing the cultured bacteria. The nanoELIwells released from the assay were dried under a vacuum for SEM analysis. The glass slides were washed and rinsed (ArrayIt Wash and Rinse Buffer) and blocked (BlockIt) for 2 hours at room temperature. This second blocking procedure with blocking buffer was applied on the glass slide. Without this second blocking step, the background might be noticeably higher. The glass slides were subsequently washed and rinsed before incubation with 2.5 μg of primary antibodies specific to the target antigen in 10 mL Reaction Buffer at room temperature for 2 hours. Another round of wash and rinse were conducted before the final incubation of the glass slides with 2.5 μg of secondary antibodies in 10 mL Reaction Buffer at room temperature for 2 hours. The slides were then subjected to the final round of wash and rinse and spun dried using a Microarray High-Speed Centrifuge. Fluorescence results were collected using a GenePix 4000B Microarray Scanner. The PDMS nanoELIwells (after drying) were visually aligned with the fluorescence images in order to better identify the area of interest for SEM imaging.



SEM imaging and bacterial counting. The nanoELIwells were guillotined into smaller pieces (if needed), sputter coated with 15 nm Au, and mounted onto stubs before imaging. A typical 3x3 mm or 5x5 mm area is scanned by capturing zoomed-in images of the wells for bacterial counting. The entire area of interest containing the bacterial sample is scanned resulting in 100 s of images per assay. These zoomed-in images are manually stitched together, as shown in Figure S1, before counting. The bacterial concentrations are reported as bacterial numbers per sample.

- Organization, W. H. Global Tuberculosis Control: WHO Report 2011. *WHO Library Cataloguing-in-Publication Data* (2011).
- Laserson, K. F. *et al.* Improved sensitivity of sputum smear microscopy after processing specimens with C18-carboxypropylbetaine to detect acid-fast bacilli: a study of United States-bound immigrants from Vietnam. *Journal of clinical microbiology* **43**, 3460–3462 (2005).
- van Ingen, J., de Zwaan, R., Dekhuijzen, R., Boeree, M. & van Soolingen, D. Region of difference 1 in nontuberculous Mycobacterium species adds a phylogenetic and taxonomical character. *Journal of bacteriology* **191**, 5865–5867 (2009).
- Wu-Hsieh, B. A. *et al.* Long-lived immune response to early secretory antigenic target 6 in individuals who had recovered from tuberculosis. *Clin Infect Dis* **33**, 1336–1340 (2001).
- Doherty, T. M. *et al.* Immune responses to the Mycobacterium tuberculosis-specific antigen ESAT-6 signal subclinical infection among contacts of tuberculosis patients. *Journal of clinical microbiology* **40**, 704–706 (2002).
- Sandgren, A. *et al.* Tuberculosis drug resistance mutation database. *PLoS medicine* **6**, e2 (2009).
- Love, J. C., Ronan, J. L., Grotenbreg, G. M., van der Veen, A. G. & Ploegh, H. L. A microengraving method for rapid selection of single cells producing antigen-specific antibodies. *Nature biotechnology* **24**, 703–707 (2006).
- Ochsner, M. *et al.* Micro-well arrays for 3D shape control and high resolution analysis of single cells. *Lab on a chip* **7**, 1074–1077 (2007).
- Moeller, H. C., Mian, M. K., Shrivastava, S., Chung, B. G. & Khademhosseini, A. A microwell array system for stem cell culture. *Biomaterials* **29**, 752–763 (2008).
- Khademhosseini, A. *et al.* Cell docking inside microwells within reversibly sealed microfluidic channels for fabricating multiphenotype cell arrays. *Lab on a chip* **5**, 1380–1386 (2005).
- Seo, J. H., Chen, L. J., Verkhoturov, S. V., Schweikert, E. A. & Revzin, A. The use of glass substrates with bi-functional silanes for designing micropatterned cell-secreted cytokine immunoassays. *Biomaterials* **32**, 5478–5488.
- Tuleuova, N. & Revzin, A. Micropatterning of Aptamer Beacons to Create Cytokine-Sensing Surfaces. *Cellular and molecular bioengineering* **3**, 337–344 (2010).
- Park, S., Han, J., Kim, W., Lee, G. M. & Kim, H. S. Rapid selection of single cells with high antibody production rates by microwell array. *J Biotechnol* **156**, 197–202 (2011).
- Han, Q., Bradshaw, E. M., Nilsson, B., Hafner, D. A. & Love, J. C. Multidimensional analysis of the frequencies and rates of cytokine secretion from single cells by quantitative microengraving. *Lab on a chip* **10**, 1391–1400 (2010).
- Jin, A. *et al.* A rapid and efficient single-cell manipulation method for screening antigen-specific antibody-secreting cells from human peripheral blood. *Nat Med* **15**, 1088–1092 (2009).
- Kim, S. H., Yamamoto, T., Fourmy, D. & Fujii, T. An electroactive microwell array for trapping and lysing single-bacterial cells. *Biomechanics* **5**, 24114 (2011).
- Rettig, J. R. & Folch, A. Large-scale single-cell trapping and imaging using microwell arrays. *Analytical chemistry* **77**, 5628–5634 (2005).
- Lecault, V. *et al.* High-throughput analysis of single hematopoietic stem cell proliferation in microfluidic cell culture arrays. *Nature methods* **8**, 581–586 (2011).
- Guldevall, K. *et al.* Imaging immune surveillance of individual natural killer cells confined in microwell arrays. *PLoS one* **5**, e15453 (2010).
- Heyries, K. A. *et al.* Megapixel digital PCR. *Nature methods* **8**, 649–651 (2011).
- Lee, W. C., Rigante, S., Pisano, A. P. & Kuypers, F. A. Large-scale arrays of picoliter chambers for single-cell analysis of large cell populations. *Lab on a chip* **10**, 2952–2958 (2010).
- Lee, H. J., Kim, H. S., Kim, H. O. & Koh, W. G. Micropatterns of double-layered nanofiber scaffolds with dual functions of cell patterning and metabolite detection. *Lab on a chip* **11**, 2849–2857 (2011).
- Han, Q. *et al.* Polyfunctional responses by human T cells result from sequential release of cytokines. *Proceedings of the National Academy of Sciences of the United States of America* **109**, 1607–1612 (2012).
- McDonald, J. C. & Whitesides, G. M. Poly(dimethylsiloxane) as a material for fabricating microfluidic devices. *Accounts of Chemical Research* **35**, 491–499 (2002).
- Belisle, J. T. *et al.* Role of the major antigen of Mycobacterium tuberculosis in cell wall biogenesis. *Science New York, N.Y.* **276**, 1420–1422 (1997).
- Wiker, H. G. & Harboe, M. The antigen 85 complex: a major secretion product of Mycobacterium tuberculosis. *Microbiol Rev* **56**, 648–661 (1992).
- Lamrabet, O., Mba Medie, F. & Drancourt, M. Acanthamoeba polyphaga-enhanced growth of Mycobacterium smegmatis. *PLoS one* **7**, e29833.
- Dhiman, R. K. *et al.* Lipoarabinomannan localization and abundance during growth of Mycobacterium smegmatis. *Journal of bacteriology* **193**, 5802–5809.
- Takayama, K. & Kilburn, J. O. Inhibition of synthesis of arabinogalactan by ethambutol in Mycobacterium smegmatis. *Antimicrobial agents and chemotherapy* **33**, 1493–1499 (1989).
- Takayama, K., Armstrong, E. L., Kunugi, K. A. & Kilburn, J. O. Inhibition by ethambutol of mycolic acid transfer into the cell wall of Mycobacterium smegmatis. *Antimicrobial agents and chemotherapy* **16**, 240–242 (1979).
- Rapaport, E., Levina, A., Metelev, V. & Zamecnik, P. C. Antimycobacterial activities of antisense oligodeoxynucleotide phosphorothioates in drug-resistant strains. *Proceedings of the National Academy of Sciences of the United States of America* **93**, 709–713 (1996).
- Lu, T. & Drlca, K. In vitro activity of C-8-methoxy fluoroquinolones against mycobacteria when combined with anti-tuberculosis agents. *The Journal of antimicrobial chemotherapy* **52**, 1025–1028 (2003).
- Chakravorty, S. *et al.* Rifampin resistance, Beijing-W clade-single nucleotide polymorphism cluster group 2 phylogeny, and the Rv2629 191-C allele in Mycobacterium tuberculosis strains. *Journal of clinical microbiology* **46**, 2555–2560 (2008).
- Ren, H. & Liu, J. AsnB is involved in natural resistance of Mycobacterium smegmatis to multiple drugs. *Antimicrobial agents and chemotherapy* **50**, 250–255 (2006).
- Hetherington, S. V., Watson, A. S. & Patrick, C. C. Sequence and analysis of the rpoB gene of Mycobacterium smegmatis. *Antimicrobial agents and chemotherapy* **39**, 2164–2166 (1995).
- Shen, G. H., Chiou, C. S., Hu, S. T., Wu, K. M. & Chen, J. H. Rapid identification of the Mycobacterium tuberculosis complex by combining the ESAT-6/CFP-10 immunochromatographic assay and smear morphology. *Journal of clinical microbiology* **49**, 902–907 (2011).
- Glassroth, J. Pulmonary disease, due to nontuberculous mycobacteria (vol 133, pg 243, 2008). *Chest* **133**, 1291–1291 (2008).
- Glassroth, J. Pulmonary disease due to nontuberculous mycobacteria. *Chest* **133**, 243–251 (2008).
- Jing, H. *et al.* Prevalence of nontuberculous mycobacteria infection, China, 2004–2009. *Emerging infectious diseases* **18**, 527–528 (2012).
- Duffy, D. C., McDonald, J. C., Schueller, O. J. A. & Whitesides, G. M. Rapid prototyping of microfluidic systems in poly(dimethylsiloxane). *Analytical chemistry* **70**, 4974–4984 (1998).

Acknowledgement

We are grateful for funding supports from CPRIT-R1007 and DOD W81XWH-11-02-0168-P8 (PI: Lidong Qin), and NIH RO1AI075465 (PI: Xin Ma). We would like to thank TMHRI SEM Core for instrument support.

Author contributions

YHN prepared Figures 1–6. YHN, XM and LQ optimized the experimental protocol and wrote the main manuscript text. All authors reviewed the manuscript.

Additional information

Supplementary information accompanies this paper at <http://www.nature.com/scientificreports>

Competing financial interests: The authors declare no competing financial interests.

License: This work is licensed under a Creative Commons Attribution-NonCommercial-ShareAlike 3.0 Unported License. To view a copy of this license, visit <http://creativecommons.org/licenses/by-nc-sa/3.0/>

How to cite this article: Nguyen, Y.H., Ma, X. & Qin, L. Rapid identification and drug susceptibility screening of ESAT-6 secreting Mycobacteria by a NanoELIwell assay. *Sci. Rep.* **2**, 635; DOI:10.1038/srep00635 (2012).